

1 **Elevated ITGA5 facilitates hyperactivated mTORC1-mediated progression of**  
2 **laryngeal squamous cell carcinoma via upregulation of EFNB2**

3 **MATERIALS AND METHODS**

4 **Tumor specimens**

5 A total of 94 LSCC and adjacent normal mucosal (ANM) tissues were acquired  
6 during routine surgeries at the First Affiliated Hospital of Anhui Medical University  
7 (Anhui, China) from 2014 to 2020. None of the patients were subjected to  
8 chemotherapy, radiotherapy, or other related antitumor therapies before surgery. The  
9 TNM staging was done referring to the American Joint Committee on Cancer (AJCC)  
10 8th edition TNM Staging Criteria. The study was conducted in accordance with  
11 Declaration of Helsinki, and the ethical approval was obtained from the First  
12 Affiliated Hospital of Anhui Medical University Research Ethics Committee. All of  
13 the patients provided a written informed consent before participation. Detailed  
14 information of all the 94 LSCC patients is listed in Table S1-4.

15 **Establishment and characterization of a novel LSCC cell line, LIU-LSC-1**

16 Fresh tumor tissue was isolated from a 74-year-old LSCC patient (T3N1M0)  
17 who underwent surgery, and the specimen was immediately immersed in RPMI 1640  
18 medium (Gibco, NY, USA) containing penicillin (100 U/mL)/streptomycin (0.1  
19 mg/mL) and amphotericin B (0.25 µg/mL) (Beyotime, Jiangsu, China). The tissue  
20 sample was washed three times in phosphate-buffered saline (PBS) and cut into small  
21 pieces. Then, small tumor masses were dissociated enzymatically in RPMI 1640

22 medium containing 200 U/mL type IV collagenase (Sigma, Saint Louis, MO, USA) at  
23 37 °C for 12 h. After two rounds of washing in PBS and centrifugation, the sediments  
24 were seeded onto 60 mm Petri dishes and cultured in Epithelial Cell Complete  
25 Medium (VivaCell, Shanghai, China) with 1% penicillin/streptomycin (Beyotime).  
26 After 3 days of incubation, the cell culture medium was replaced. Cells were passaged  
27 every 3 to 4 days. Cancer-associated fibroblasts (CAFs) were removed by a brief  
28 exposure to trypsin digestion (0.25% trypsin-EDTA, Beyotime). Cells were named  
29 LIU-LSC-1 and compared with the short-tandem repeat (STR) data of cell lines  
30 included in ATCC, DSMZ, JCRB and RIKEN databases. No closely matched cell  
31 lines were found (Table S5,  $EV < 0.8$ ), which suggested that LIU-LSC-1 may be a  
32 new cell line. Mycoplasma analysis of this cell line was negative.

33 For Giemsa staining, followed by fixation with methanol for 10 min, LIU-LSC-1  
34 cells were stained with crystal violet for 10 min and photographed under microscope.  
35 Ultrastructural analysis of cells was performed by transmission electron microscopy  
36 (TEM). In brief, LIU-LSC-1 cells were fixed with 2.5% glutaraldehyde at 4 °C for 2.5  
37 h, and then the cells were washed three times with PBS and post-fixed in 1% OsO<sub>4</sub> for  
38 2 h at 4 °C. After being dehydrated through an ethanol gradient, the samples were  
39 embedded in Spurr's resin. Then ultrathin sections were cut and stained with either  
40 uranyl acetate or lead citrate. The samples were observed under a JEOL JEM1400  
41 TEM. Tonofilaments in the cytoplasm, desmosomes in the intercellular connections,  
42 intranuclear inclusions and indented nuclear membrane are supposed to the  
43 characteristics of tumor cells [1].

44 For flow cytometry, LIU-LSC-1 cells at the logarithmic growth phase were  
45 stained with CD44 (5  $\mu\text{g}/\text{mL}$ ) or the isotype control antibodies (5  $\mu\text{g}/\text{mL}$ ) for 30 min  
46 at room temperature in the dark. After washed three times by  
47 centrifugation-resuspension with ice-cold PBS, the cells were stained with a  
48 secondary antibody (Goat Anti-Mouse IgG H&L, DyLight® 488) and incubated for  
49 30 min. Subsequently, the cells were analyzed by flow cytometer (Becton Dickinson,  
50 San Diego, CA, USA).

## 51 **Cell culture**

52 Cell source and culture conditions of murine embryonic fibroblasts (MEFs)  
53 ( $\text{Tsc1}^{+/+}$ ,  $\text{Tsc1}^{-/-}$ ,  $\text{Tsc2}^{+/+}$ , and  $\text{Tsc2}^{-/-}$ ), HEK293T cells and LSCC cell lines  
54 (AMC-HN-8, TU177, and LIU-LSC-1) are listed in Table S6. MEFs ( $\text{Tsc1}^{+/+}$ ,  $\text{Tsc1}^{-/-}$ ,  
55  $\text{Tsc2}^{+/+}$ , and  $\text{Tsc2}^{-/-}$ ) have been described previously [2, 3]. For hypoxic exposure,  
56 cells were cultured under hypoxic (1%  $\text{O}_2$ ) or normoxic (21%  $\text{O}_2$ ) conditions for the  
57 indicated times. All cell lines were verified by STR analysis and tested for  
58 mycoplasma contamination by MycoAlert Mycoplasma Detection Kit (Lonza  
59 #LT07-118).

## 60 **Antibodies, reagents and plasmids**

61 All information regarding antibodies used in this study is provided in Table 7.  
62 Rapamycin (Rapa), everolimus (RAD001), deferoxamine (DFX), DAPT and  
63 MHY1485 were purchased from Selleck Chemicals (Houston, TX, USA). Jagged1-Fc  
64 was obtained from R&D system (Minneapolis, MN, USA). Lipofectamine RNAiMax

65 was obtained from Invitrogen (Carlsbad, CA, USA). pRL-TK, pGL3-Basic,  
66 pcDNA3.0, pcDNA3.0-HA-HIF-1 $\alpha$ , lenti-CRISPRv2 plasmids and packaging vectors  
67 (pVSVG and psPAX2) were purchased from Addgene (Cambridge, MA, USA).

## 68 **RNA interference, lentivirus infection and CRISPR-Cas9**

69 LIU-LSC-1 cells were seeded into 12-well plates and transfected with small  
70 interfering RNAs (siRNAs) using Lipofectamine RNAiMax (GenePharma, Shanghai,  
71 China). The sequences used are as follows: mTOR  
72 5'-CCCUGCCUUUGUCAUGCCUTT-3'; Rictor,  
73 5'-ACUUGUGAAGAAUCGUAUCTT-3'; Raptor,  
74 5'-GGACAACGGCCACAAGUACTT-3'; Negative control (NC),  
75 5'-UUCUCCGAACGUGUCACGUTT-3'.

76 LIU-LSC-1 cells were stably infected with short hairpin RNAs (shRNAs)  
77 targeting HIF-1 $\alpha$ , Raptor, ITGA5 and EFNB2 using lentivirus vector GV248  
78 (GenePharma). The target sequences used are as follows: shRaptor-1,  
79 5'-GGACAACGGCCACAAGTAC-3'; shRaptor-2,  
80 5'-CCCTCATCGGAGTTTCCTT-3'; shHIF-1 $\alpha$ -1, 5'-GCCGCTCAATTTATGAATA-3';  
81 shHIF-1 $\alpha$ -2, 5'-GCTGGAGACACAATCATAT-3'; shITGA5,  
82 5'-GCTACCTCTCCACAGATAACT-3'; shEFNB2-1,  
83 5'-GCAGAACTGCGATTTCCAAAT-3'; shEFNB2-2,  
84 5'-GGAATTCCTCGAACTCCAAAT-3'; the control scrambled shRNA (shSc),  
85 5'-TTCTCCGAACGTGTCACGT-3'. The recombinant vectors were co-transfected  
86 with packing vectors (psPAX2 and pVSVG) into HEK293T cells. After 48 h, the viral

87 supernatants were filtered and used to infect LIU-LSC-1 cells. ITGA5 and EFNB2  
88 overexpressing cell lines were generated by lentivirus vector GV492 containing the  
89 full-length cDNA sequence of human ITGA5 and EFNB2, respectively  
90 (GenePharma).

91 The following single-guide RNAs (sgRNAs) targeting ITGA5 and TSC2 were  
92 designed by Open-access software program CRISPR and synthesized by Sangon  
93 Biotech Co., Ltd. (Shanghai, China): ITGA5-sgRNA#1,  
94 5'-GGGGCAACAGTTCGAGCCCA-3'; ITGA5-sgRNA#2,  
95 5'-GGAGCCACTGAGCGACCCCG-3'; TSC2-sgRNA,  
96 5'-CACCGAACAATCGCATCCGGATGAT-3'. Oligos were then cloned into the Cas9  
97 backbone Lenti-CRISPRv2 vector. Recombinant plasmids, psPAX2 and pVSVG were  
98 co-transfected into HEK293T cells. The medium was harvested and filtered to remove  
99 cell debris 48 h later. After infection, the cells were obtained by culture over 14 days  
100 in 1.5 µg/mL puromycin (Sigma, MO, USA). Then cells were placed in 96-well plates  
101 and examined by microscopy the next day to be sure that only one cell was seeded per  
102 well. Clones were passaged after 10 days and monoclonal lines were screened via  
103 western blotting for ITGA5 knockout.

#### 104 **Total RNA isolation, quantitative real-time PCR (qRT-PCR) assay and RNA** 105 **sequencing**

106 Total RNA extraction, cDNA synthesis, qRT-PCR and RNA sequencing were  
107 performed as described previously [4]. The primers for qRT-PCR (provided by

108 Sangon Biotech Co., Ltd.) are shown in Table S8. The RNA samples were sequenced  
109 on Illumina Novaseq™ 6000 (LC Sciences, Hangzhou, China).

#### 110 **Western blot analysis**

111 The total protein of cells was harvested using RIPA lysate (Beyotime). The  
112 lysates were separated by NuPAGE 4-12% Bis-Tris and transferred to polyvinylidene  
113 fluoride membrane (Millipore, Billerica, MA, USA). Then the membrane was blocked  
114 with 5% nonfat milk for 1 h and incubated with the primary antibodies (diluted 1:  
115 1000) at 4 °C overnight. Final detection was performed using chemiluminescence  
116 after the secondary antibody incubation.

#### 117 **Chromatin immunoprecipitation (ChIP)**

118 The ChIP assay was performed as previously described using a SimpleChIP®  
119 Plus Enzymatic Chromatin IP Kit (Cell Signaling Technology, MA, USA) [5]. PCR  
120 primer sequences for the putative HIF-1 $\alpha$ -binding region (PBR) and a nonspecific  
121 HIF-1 $\alpha$ -binding region (NBR) of human ITGA5 were as follows: Site1, forward,  
122 5'-CCACCCCTAATCTCCCAAATCCT-3'; reverse,  
123 5'-TCAGGATCTTTAAGCCCAGCATTG-3'; Site2, forward,  
124 5'-CCAAACCCGCCAGTCTAACC-3'; reverse, 5'-GGGGGGGCATTCCTGGGT-3';  
125 NBR, forward, 5'-CAAAGCCAGCACCAGTGAAGAGAC-3'; reverse,  
126 5'-CCCTCCTCCCAACACACACATATATAC-3'. The primer sequences for qRT-PCR  
127 were as follows: NBR, forward, 5'-AAGCCAGCACCAGTGAAGAGAC-3'; reverse,  
128 5'-ACTCCTGGTTCTAGCTACTTTAATCAC-3'. PBR, forward,

129 5'-CGCCCAGTCTAACCCAGTCCA-3'; reverse,

130 5'-CCTGGGTCCCTGGAAGTCTGAG-3'.

### 131 **Reporter constructs and luciferase reporter assay**

132 A 334-bp fragment of the human ITGA5 promoter (-266/+67) containing the

133 intact HIF-1 $\alpha$ -binding site was obtained by PCR using human genomic DNA. The

134 primer sequences were as follows: forward,

135 5'-GGGGTACCTGGAAAGGAATGGGGAGGAAGGAG-3'; reverse,

136 5'-GAAGATCTGCGCCCGCTCTTCCCTGTCC-3'. The fragment was cloned into the

137 *Bgl* II and *Kpn* I sites of the pGL3-Basic plasmid (ITGA5-Luc). A Q5<sup>®</sup> Site-Directed

138 Mutagenesis Kit (NEB, Ipswich, MA, USA) was used to mutate the potential

139 HIF-1 $\alpha$ -binding site (ITGA5-mut). The primer sequences were as follows: forward,

140 5'-CCCCTAAGGGAAATGGGGGGGGGGCGC-3'; reverse,

141 5'-TGGGGGACGCGGGCTCAG -3'. The 293T cells were then seeded into 24-well

142 culture plates and transfected with 400 ng of ITGA5-Luc or ITGA5-mut together with

143 20 ng of an internal control plasmid pRL-TK and 400 ng of HA-HIF-1 $\alpha$ -pcDNA3.0 or

144 the empty vector pcDNA3.0. The luciferase activity was estimated using the

145 Dual-Luciferase Reporter Assay System (Promega, USA).

### 146 ***In vitro* functional assays**

147 Cell Counting Kit-8 (CCK-8, TargetMol, Shanghai, China), colony formation,

148 wound healing and transwell assays were used to test the *in vitro* functional roles of

149 ITGA5 and EFNB2. For CCK-8 assay, cells were seeded onto 96-well plates with

150 indicated treatment at 1000 cells/well. 10  $\mu$ L of CCK-8 reagent was added to each  
151 well at the specified time point. After incubation for 2 h, the reaction product was  
152 measured at 450 nm using a microplate reader. For colony formation assays, 1500 of  
153 treated cells were seeded into 60 mm plates. 10 days later, cells were fixed with 4%  
154 paraformaldehyde and stained with crystal violet. Colonies containing more than 50  
155 cells were counted. For wound healing assay, in order to create a narrow wound-like  
156 gap, the monolayer of cells was scratched with a 200- $\mu$ L pipette tip. Cell migration  
157 into the wound area was recorded for each condition after 18 h or 24 h. For transwell  
158 assays, 24-well transwell chambers (Corning, NY, USA) were used.  $2 \times 10^4$  cells in  
159 200  $\mu$ L of DMEM (or RPMI 1640) with 1% FBS were seeded in the upper chamber  
160 and the lower chamber contained 500  $\mu$ L medium with 10% FBS. The chambers were  
161 incubated at 37  $^{\circ}$ C with 5% CO<sub>2</sub> for 24 h (migration assay, without matrigel; invasion  
162 assay, coated with 250  $\mu$ g/mL matrigel coating). Then, cells on the upper surface of  
163 the filter were removed and the cells on the lower membrane surface were stained  
164 with crystal violet after fixation with 4% paraformaldehyde. Cell migration and  
165 invasion were quantified by counting 10 random fields under a microscope (200 $\times$ ).

#### 166 **Chicken chorioallantoic membrane (CAM) assay**

167 Pathogen-free fertilized chicken eggs were purchased from Jinan SAIS Poultry  
168 Company (Shangdong, China). The CAM assay was performed as described  
169 previously [6]. Briefly, On embryonic developmental day 8 (EDD 8), a window about  
170 1.0 cm was opened in the shell of each egg, and sterile gelatin sponge mixed with 20  
171  $\mu$ L of cell suspension containing  $2 \times 10^6$  LSCC cells was planted on CAM. The CAM

172 was separated from the eggs after fixation with stationary solution (methanol: acetone,  
173 1:1) for 30 min on EDD 15. Then, the CAM was recorded by a digital camera, and the  
174 number of blood vessels that converged toward the implant were counted by three  
175 blind observers.

### 176 **Animal experiments, cell derived xenograft (CDX) models and patient-derived** 177 **xenograft (PDX) models**

178 All animal studies were performed under approval of the Experimental Animal  
179 Ethical Committee of Anhui Medical University. Male BALB/c nude mice and  
180 NOD/SCID mice (4-week-old) were purchased from GemPharmatech Co., Ltd  
181 (Nanjing, China). For tumorigenicity assays,  $5 \times 10^6$  genetically engineered LSCC  
182 cells were subcutaneously injected into the right armpits of each mice (five per group),  
183 respectively. The tumor volume was measured and calculated by the formula  $V = 0.5$   
184  $\times W^2 \times L$  (V, volume; L, length; W, width).

185 For tumor metastasis experiments,  $1 \times 10^6$  genetically engineered LSCC cells  
186 suspended in 100  $\mu$ L PBS were injected into nude mice via the tail vein. Mice were  
187 killed and metastatic lung tumors were analyzed under dissecting microscope after  
188 hematoxylin and eosin (H&E) staining at 8 weeks after tail vein injection.

189 For intratumoral siRNAs injections, the chemically modified siRNAs were  
190 provided by GenePharma. The target sequences are listed as follows: siNC,  
191 5'-UUCUCCGAACGUGUCACGUTT-3'; siITGA5-1,  
192 5'-UACCUCUCCACAGAUAACUTT-3'. Entranster<sup>TM</sup>-*in vivo* transfection reagents  
193 were provided by Engreen Biosystem Co., Ltd (Beijing, China).

194 For CDX models, 200  $\mu$ L serum-free RPMI 1640 containing  $5 \times 10^6$  LIU-LSC-1  
195 cells were subcutaneously injected into the right flank of each mouse. After tumors  
196 were detectable, 20 tumor-bearing mice were randomly assigned into four groups  
197 (five per group) and were treated with CDDP (3 mg/kg, twice/week), normal saline  
198 (NS, twice/week), together with ITGA5 siRNAs (100  $\mu$ g, twice/week) or  
199 non-targeting control siRNAs (100  $\mu$ g, twice/week). siRNA was injected directly into  
200 the tumor bodies at two or more spots each time. NS and CDDP were injected into the  
201 abdominal cavity. The mice were sacrificed after 3 weeks of treatment, and then  
202 tumors were dissected and weighed. Furthermore, tissues were embedded in paraffin  
203 for H&E or IHC.

204 For PDX models, freshly excised tumor tissues were obtained from a LSCC  
205 patient receiving surgery at the First Affiliated Hospital of Anhui Medical University.  
206 The tissues were cut into  $2 \times 2 \times 3$ -mm<sup>3</sup> pieces (kept in PRMI 1640 supplemented  
207 with penicillin and streptomycin) and grafted subcutaneously into the flank of  
208 NOD/SCID mice as P1. PDX tumors were harvested and transplanted into BALB/c  
209 nude mice as P2 when the tumor size upon reached a size of 1000 mm<sup>3</sup>. We followed  
210 the aforementioned protocols to transplant PDX tumor tissues into next-generation  
211 mice as P3 and performed next step according to the protocol of CDX models.

## 212 **Immunohistochemical staining (IHC) and immunofluorescence (IF) assay**

213 IHC analysis staining was performed as previously described [5]. Antibodies  
214 against ITGA5 (diluted 1:50), EFNB2 (diluted 1:200), p-S6 (diluted 1:75), Ki-67  
215 (diluted 1:100) and CD31 (diluted 1:100) were used. A modified histologic score

216 (H-scores, [ $\{\% \text{ of weak staining}\} \times 1$ ] + [ $\{\% \text{ of moderate staining}\} \times 2$ ] + [ $\{\% \text{ of}$   
217  $\text{strong staining}\} \times 3$ ]) was used to evaluate IHC staining [7, 8]. Each staining obtained  
218 an H-score between 0 and 300, and the average of H-score for all the cases was  
219 calculated.

220 For IF assays, Cells were treated with DMSO, Rapa (20 nM), RAD001 (50 nM)  
221 or MHY1485 (10  $\mu$ M) for 24 h and then stained as previously described [5]. Primary  
222 antibodies against ITGA5 (diluted 1:50), EFNB2 (diluted 1:200), or CD44 (diluted  
223 1:1000) and FITC-conjugated secondary antibody (diluted 1:1000) were used. DAPI  
224 (Beyotime) was used to stain nuclei. The images were captured by LSM880 +  
225 Airyscan confocal laser scanning microscope (Carl Zeiss, Oberkochen, Germany).

## 226 **Bioinformatics analysis and Statistical analysis**

227 RNA sequencing data and clinical information of LSCC were obtained from the  
228 Gene Expression Omnibus (GEO) dataset (<http://www.ncbi.nlm.nih.gov/geo/>) and  
229 The Cancer Genome Atlas (TCGA) (<http://cancergenome.nih.gov/>). The receiver  
230 operating characteristic (ROC) curves were used to evaluate the sensitivity and  
231 specificity of genes as diagnostic biomarkers.

232 All statistical analyses were performed using GraphPad Prism 6.0. Differences  
233 between two experimental groups were conducted using the two-tailed Student's t-test.  
234 Correlations between genes were analyzed by Pearson's correlation analysis. The  
235 survival rates were calculated by the Kaplan-Meier method.  $P < 0.05$  was considered  
236 statistically significant (\* $P < 0.05$ , \*\* $P < 0.01$  and \*\*\* $P < 0.001$ ).

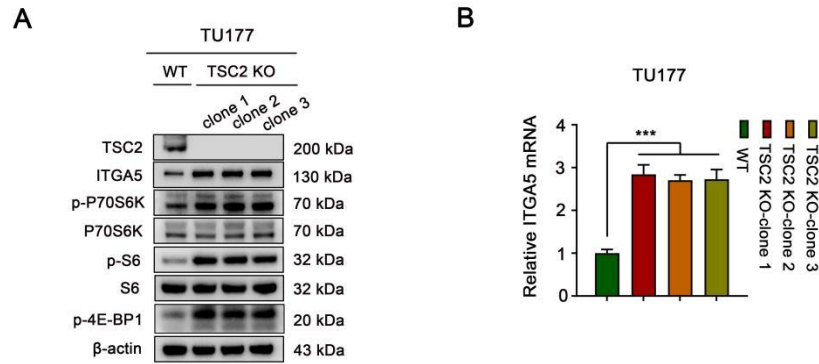
237 **References**

- 238 1. Wu CP, Zhou L, Gong HL, Du HD, Tian J, Sun S, et al. Establishment and characterization of a novel  
239 HPV-negative laryngeal squamous cell carcinoma cell line, FD-LSC-1, with missense and nonsense  
240 mutations of TP53 in the DNA-binding domain. *Cancer letters*. 2014; 342: 92-103.
- 241 2. Zhang H, Bajraszewski N, Wu E, Wang H, Moseman AP, Dabora SL, et al. PDGFRs are critical for  
242 PI3K/Akt activation and negatively regulated by mTOR. *The Journal of clinical investigation*. 2007; 117:  
243 730-8.
- 244 3. Zha X, Wang F, Wang Y, He S, Jing Y, Wu X, et al. Lactate dehydrogenase B is critical for  
245 hyperactive mTOR-mediated tumorigenesis. *Cancer research*. 2011; 71: 13-8.
- 246 4. Wang YN, Xu YF, Liang YX, Fan XY, Zha XJ. Transcriptomic Sequencing of Airway Epithelial Cell  
247 NCI-H292 Induced by Synthetic Cationic Polypeptides. *BioMed research international*. 2019; 2019:  
248 3638469.
- 249 5. Wan X, Zhou M, Huang F, Zhao N, Chen X, Wu Y, et al. AKT1-CREB stimulation of PDGFR $\alpha$   
250 expression is pivotal for PTEN deficient tumor development. *Cell Death Dis*. 2021; 12: 172.
- 251 6. Chen X, Miao M, Zhou M, Chen J, Li D, Zhang L, et al. Poly-L-arginine promotes asthma  
252 angiogenesis through induction of FGFBP1 in airway epithelial cells via activation of the  
253 mTORC1-STAT3 pathway. *Cell Death Dis*. 2021; 12: 761.
- 254 7. Detre S, Saclani Jotti G, Dowsett M. A "quickscore" method for immunohistochemical  
255 semiquantitation: validation for oestrogen receptor in breast carcinomas. *J Clin Pathol*. 1995; 48:  
256 876-8.
- 257 8. Paschalis A, Sheehan B, Riisnaes R, Rodrigues DN, Gurel B, Bertan C, et al. Prostate-specific  
258 Membrane Antigen Heterogeneity and DNA Repair Defects in Prostate Cancer. *Eur Urol*. 2019; 76:  
259 469-78.

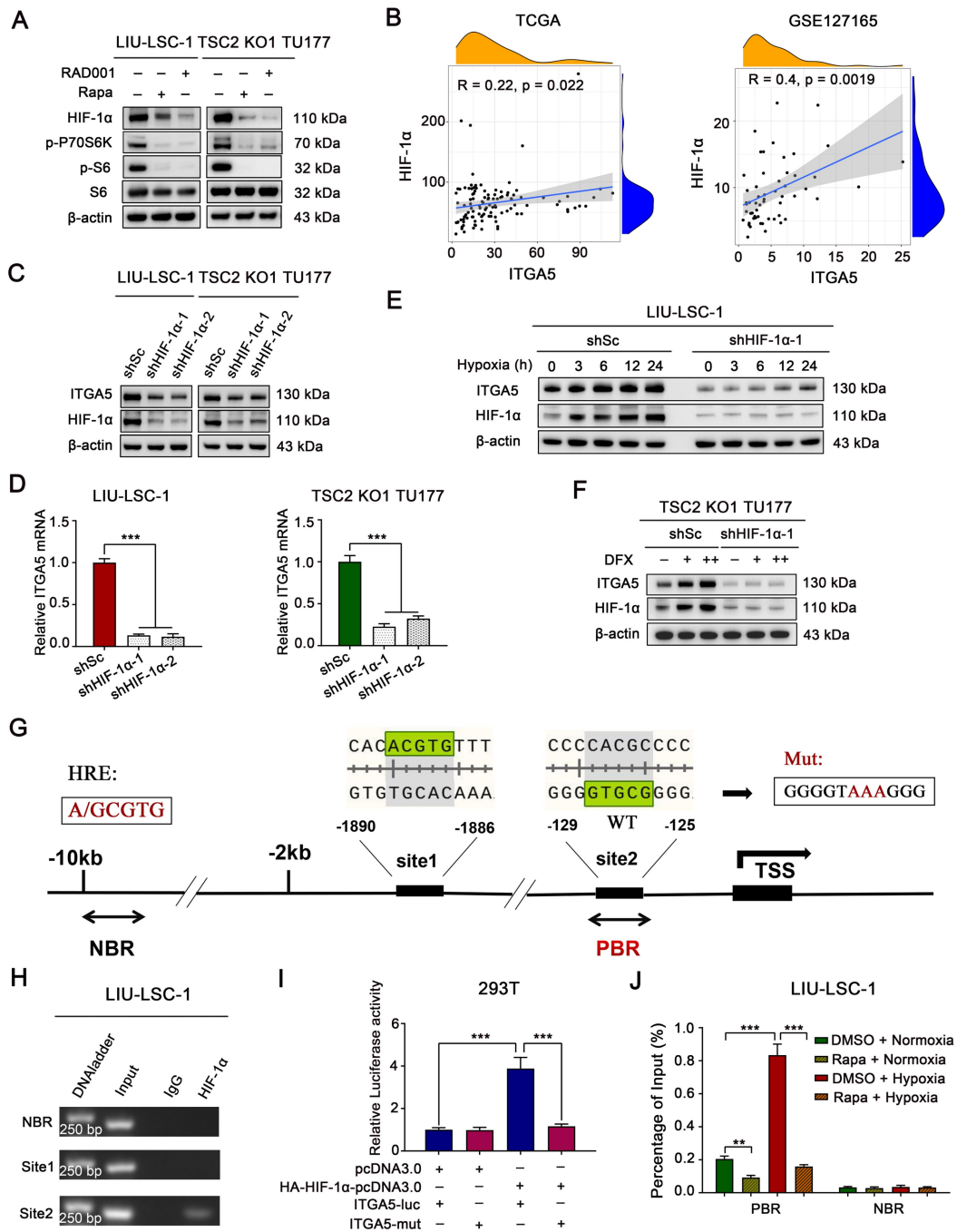
260

## SUPPLEMENTARY FIGURES

261 **Figure S1**

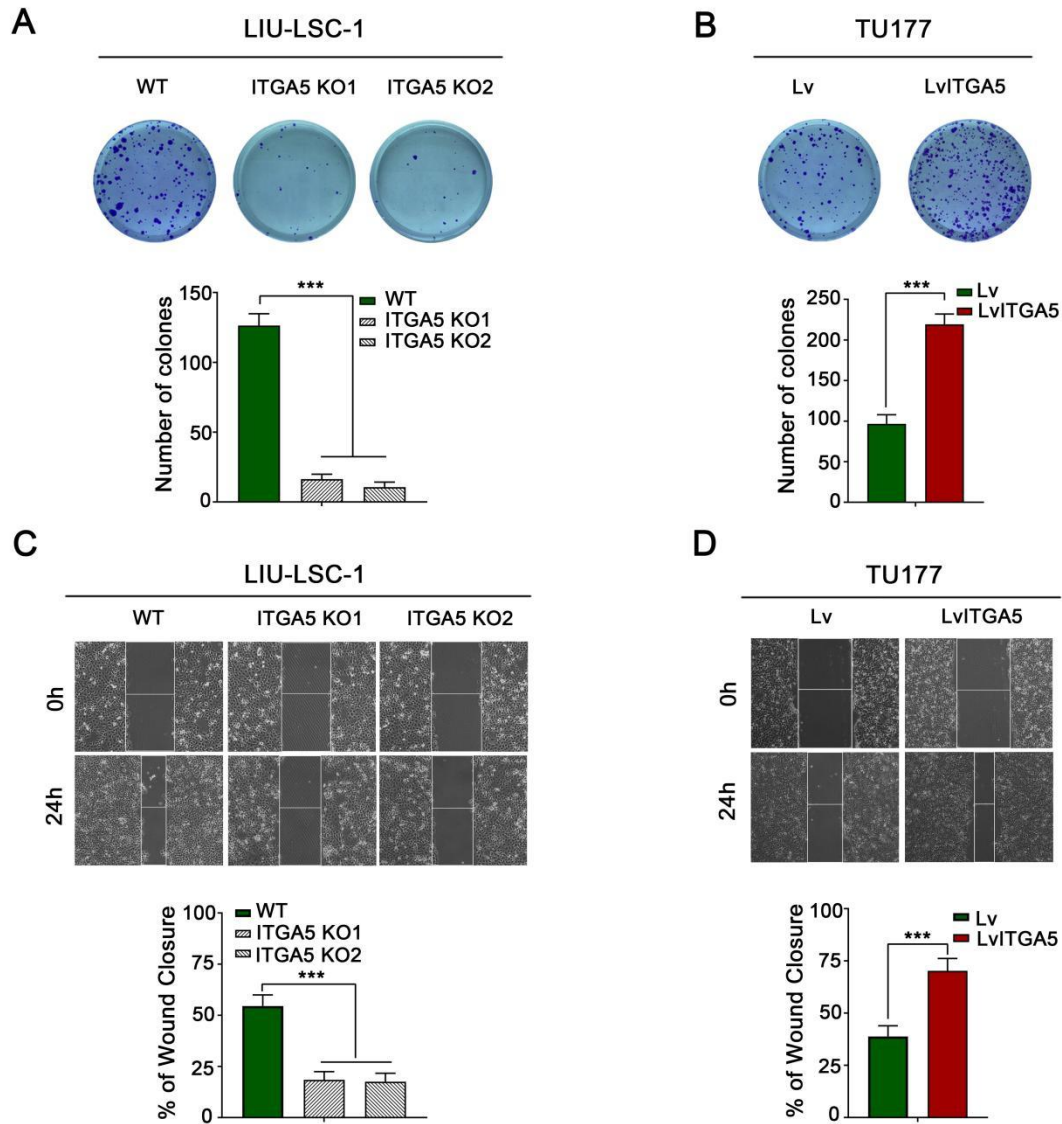


262 **Figure S1. Knockout of TSC2 led to the activation of mTORC1 and the**  
263 **upregulation of ITGA5 in the TU177 cells. (A-B) TSC2 knockout TU177 cell lines**  
264 were constructed using a CRISPR/Cas9 approach and three different clones were  
265 screened out. Cell lysates of the indicated cells were subjected to western blotting  
266 with the indicated antibodies (A). ITGA5 mRNA levels in the indicated cells were  
267 detected using qRT-PCR (B). The error bars represent the mean  $\pm$  SD of triplicate  
268 technical replicates. \*\*\*P < 0.001.



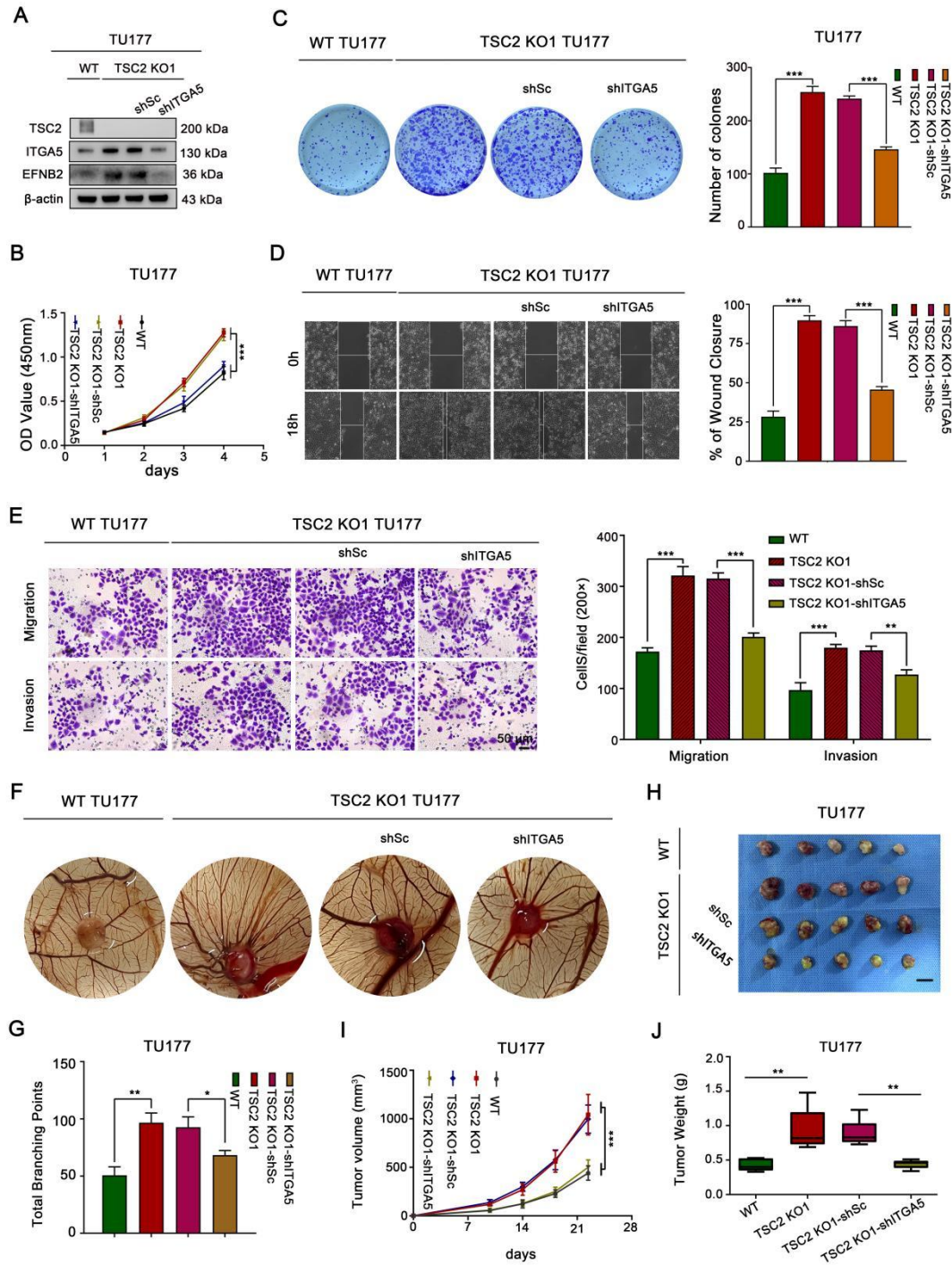
270 **Figure S2. mTORC1 enhances ITGA5 expression through upregulation of**  
 271 **HIF-1 $\alpha$ .** (A) LIU-LSC-1 and TSC2 KO1 TU177 cells were treated with 20 nM Rapa  
 272 or 50 nM RAD001 for 24 h, and cell lysates were subjected to western blot analysis.  
 273 (B) The correlation between HIF-1 $\alpha$  and ITGA5 expression was analyzed by

274 Pearson's correlation analysis using the TCGA and GSE127165 cohorts. **(C-D)**  
275 LIU-LSC-1 and TSC2 KO1 TU177 cells were transfected with shRNAs targeting  
276 HIF-1 $\alpha$  (shHIF-1 $\alpha$ ) or control shRNA- (shSc). Immunoblotting **(C)** and qRT-PCR **(D)**  
277 were performed to detect the expression of ITGA5. **(E-F)** LIU-LSC-1-shHIF-1 $\alpha$  and  
278 LIU-LSC-1-shSc cells were treated with 1% O<sub>2</sub> for the indicated times **(E)**;  
279 HIF-1 $\alpha$ -knockdown TSC2 KO1 TU177 cells and the control cells were treated with  
280 DFX (+ indicates 100  $\mu$ M; ++ indicates 200  $\mu$ M) for 24 h **(F)**. Cell lysates were  
281 subjected to western blot analysis **(E-F)**. **(G)** Schematic representation of the putative  
282 HIF-1-binding site of the human *ITGA5* gene. **(H)** LIU-LSC-1 cells were subjected to  
283 ChIP assay using an anti-HIF-1 $\alpha$  antibody. Normal rabbit IgG antibody was used as a  
284 negative control. PCR amplifications were performed using primers surrounding the  
285 putative HIF-1 $\alpha$  binding site of the human *ITGA5* gene. **(I)** The ITGA5-Luc or  
286 ITGA5-mut constructs together with HA-HIF-1 $\alpha$ -pcDNA3.0 or pcDNA3.0 were  
287 co-transfected into the 293T cells with pRL-TK plasmid for 24 h, and then luciferase  
288 activity was estimated. **(J)** LIU-LSC-1 cells were treated with DMSO or 20 nM Rapa  
289 under normoxia or hypoxia condition for 24 h. HIF-1 $\alpha$  antibody-immunoprecipitated  
290 DNA from these cells was amplified and quantified by qRT-PCR for NBR and PBR  
291 regions. The data were plotted as the ratio of immunoprecipitated DNA subtracting  
292 nonspecific binding to IgG vs. total input DNA (%). The error bars represent the mean  
293  $\pm$  SD of triplicate technical replicates. \*\*\*P < 0.001.



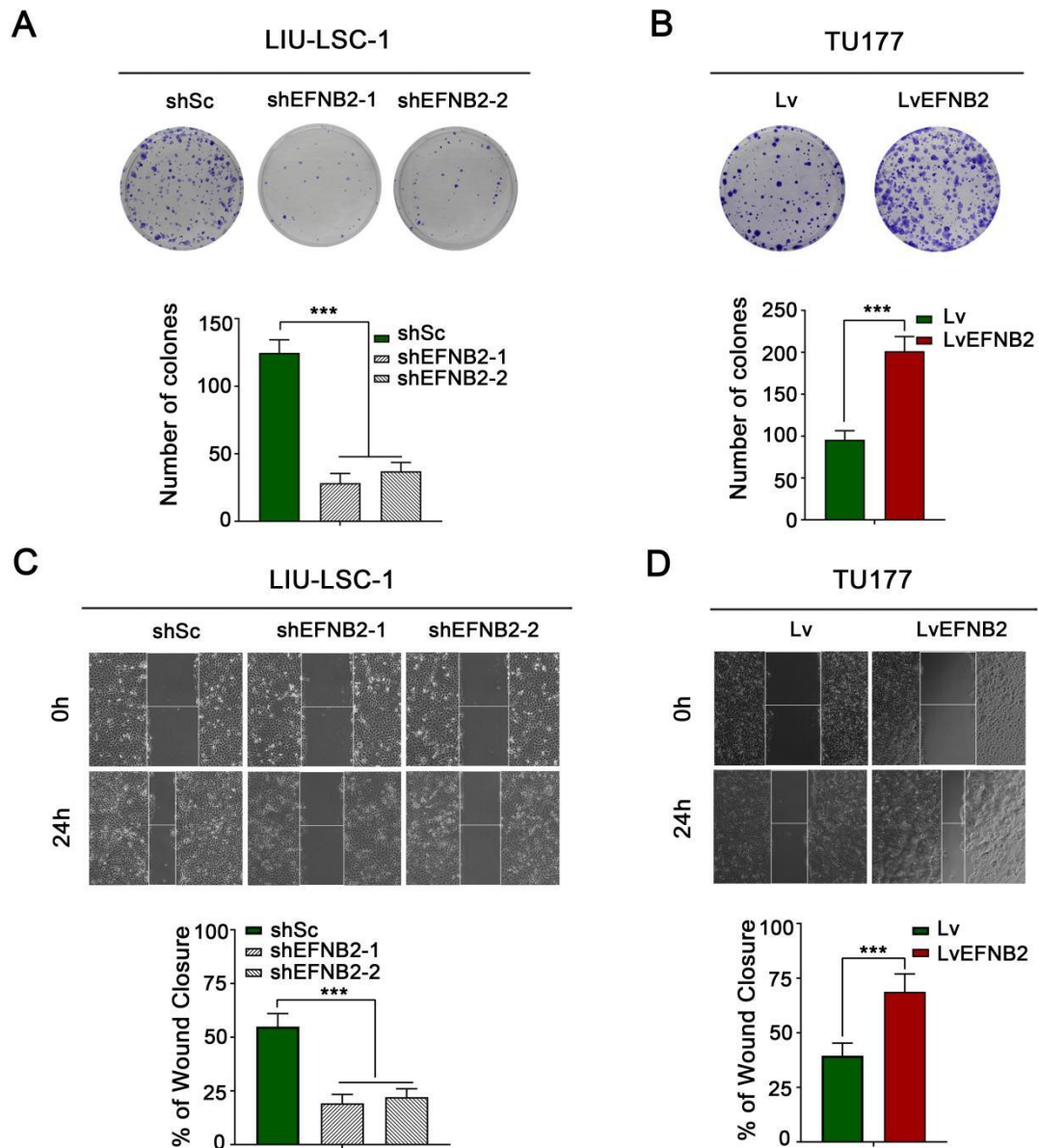
295 **Figure S3. ITGA5 promotes proliferation and migration of LSCC cells. (A, C)**  
 296 ITGA5 WT and KO LIU-LSC-1 cells. **(B, D)** ITGA5-overexpressing TU177 cells and  
 297 the control cells. Proliferative and migratory abilities of the indicated cells were  
 298 measured by colony formation **(A-B)** and wound healing assays **(C-D)**, respectively.  
 299 The error bars represent the mean  $\pm$  SD of triplicate independent experiments. \*\*\*P <  
 300 0.001.

301 **Figure S4**

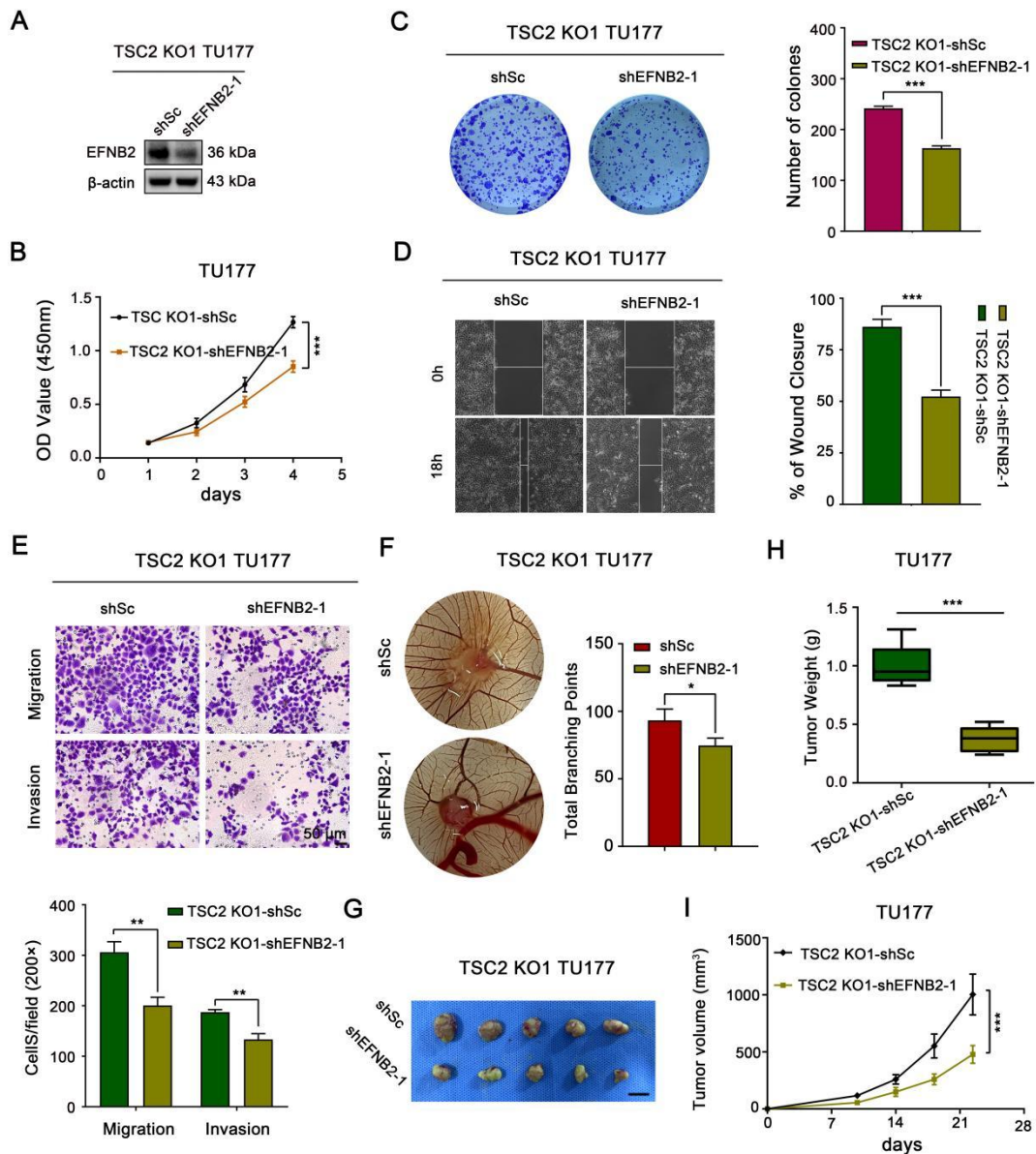


302 **Figure S4. Depletion of ITGA5 reduced the tumor-promoting effect of TSC2**  
 303 **knockout on the TU177 cells. (A-J) TSC2 KO1 TU177 cells were infected with**  
 304 **ITGA5 shRNAs-expressing (shITGA5) lentiviruses or shSc. Cell lysates of the**  
 305 **indicated cells were subjected to western blotting (A). Cell growth rates, migration**

306 and invasion abilities of the indicated cells were evaluated by CCK-8 assays **(B)**,  
307 colony formation assays **(C)**, wound healing assays **(D)** and transwell assays **(E)**,  
308 **(C-E, left panel: representative images; right panel: statistical analysis)**. Scale bars,  
309 50  $\mu\text{m}$ . Data were indicated as mean  $\pm$  SD of triplicate technical replicates. \*\*P < 0.01,  
310 \*\*\*P < 0.001. The indicated cells were subjected to CAM assays **(F-G)**,  
311 representative images **(F)** and statistical analysis **(G)** are shown. The error bars  
312 represent mean  $\pm$  SD (n = 6 per group). \*P < 0.05; \*\*P < 0.01. **(H-J)** The indicated  
313 cells were subcutaneously injected into mice for monitoring tumor growth. The tumor  
314 images **(H)**, tumor volumes **(I)** and tumor weights **(J)** were shown. Error bars indicate  
315 mean  $\pm$  SD (n = 5 mice/group). \*\*P < 0.01, \*\*\*P < 0.001. Scale bars, 1 cm **(H)**.



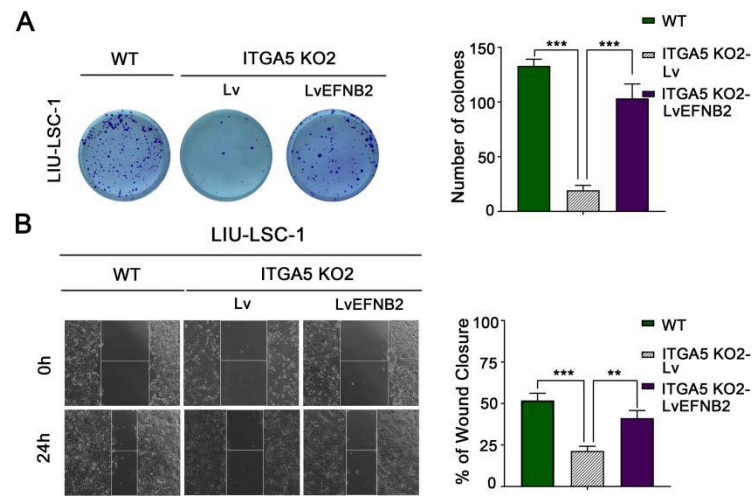
317 **Figure S5. EFNB2 promotes LSCC cells proliferation and migration. (A, C)**  
 318 EFNB2 shRNA-expressing (shEFNB2-1 or shEFNB2-2) LIU-LSC-1 cells and their  
 319 control cells (shSc). **(B, D)** EFNB2-overexpressing (LvEFNB2) TU177 cells and their  
 320 counterpart control cells (Lv). Cell proliferation was determined by colony formation  
 321 assay **(A-B)**. Cell migration was assessed by wound healing assay **(C-D)**. The error  
 322 bars represent the mean  $\pm$  SD of triplicate independent experiments. \*\*\*P < 0.001.



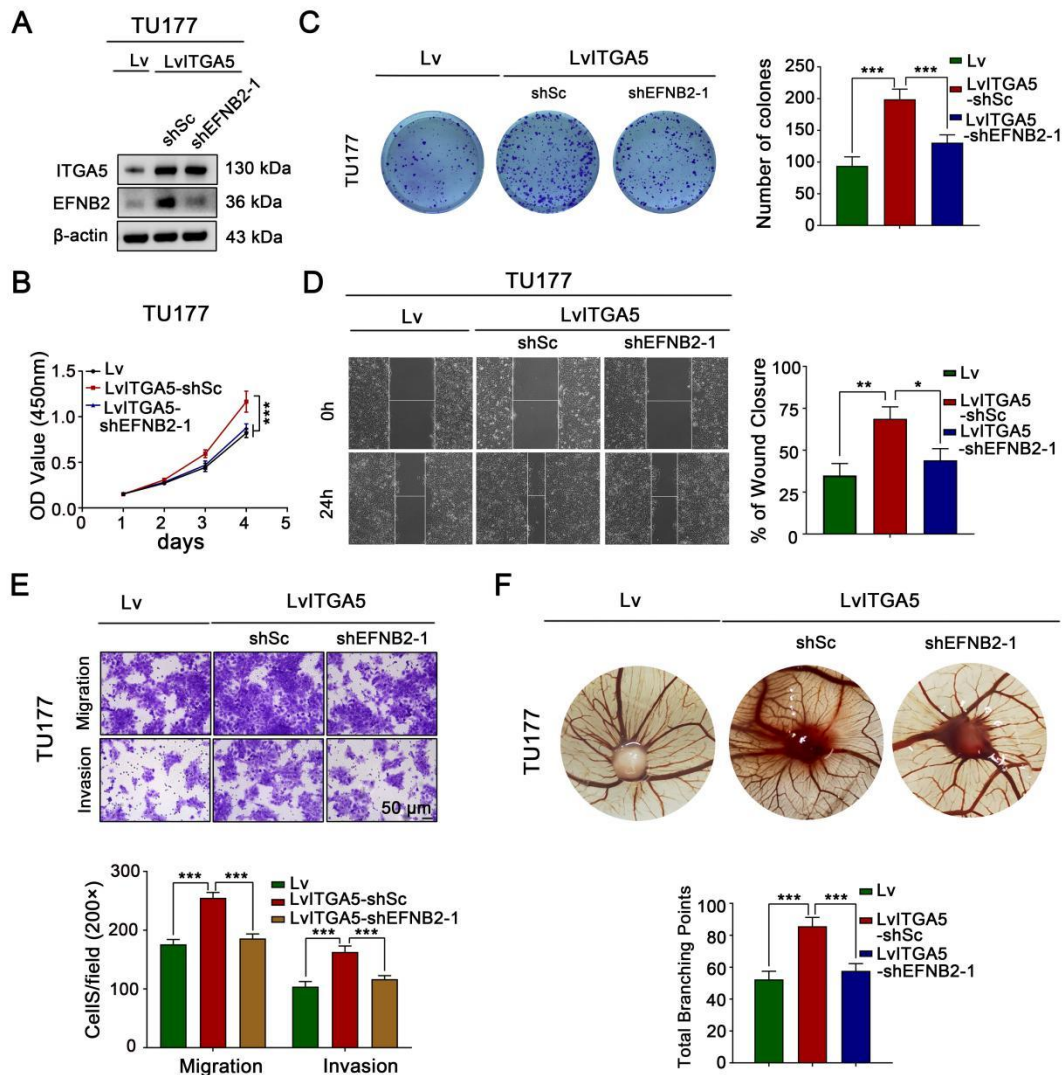
324 **Figure S6. Silencing of EFNB2 reduced the proliferation, migration, invasion,**  
 325 **angiogenesis and tumor growth abilities of the TSC2 KO1 TU177 cells. (A-I) The**  
 326 **TSC2 KO1 TU177 cells were infected with EFNB2 shRNAs-expressing (shEFNB2-1)**  
 327 **or control shRNA- (shSc) lentiviruses. The EFNB2 expression was assessed using**  
 328 **western blotting (A). Cell growth rates, migration and invasion abilities of the**  
 329 **indicated cells were evaluated by CCK-8 assays (B), colony formation assays (C, left**

330 **panel:** representative images; **right panel:** statistical analysis), wound healing assays  
331 (**D, left panel:** representative images; **right panel:** statistical analysis) and transwell  
332 assays (**E, upper panel:** representative images; **lower panel:** statistical analysis).  
333 Scale bars, 50  $\mu\text{m}$ . Data were indicated as mean  $\pm$  SD of triplicate technical replicates.  
334 **\*\*P < 0.01, \*\*\*P < 0.001.** The indicated cells were subjected to CAM assays (**F, left**  
335 **panel:** representative images; **right panel:** statistical analysis). The error bars  
336 represent mean  $\pm$  SD (n = 6 per group). \*P < 0.05. (**G-I**) The indicated cells were  
337 subcutaneously injected into mice for monitoring tumor growth. The tumor images (**G**)  
338 were recorded. The tumor weights (**H**) and tumor volumes (**I**) were quantified. Error  
339 bars indicate mean  $\pm$  SD (n = 5 mice/group). **\*\*\*P < 0.001.** Scale bars, 1 cm (**G**).

340 **Figure S7**

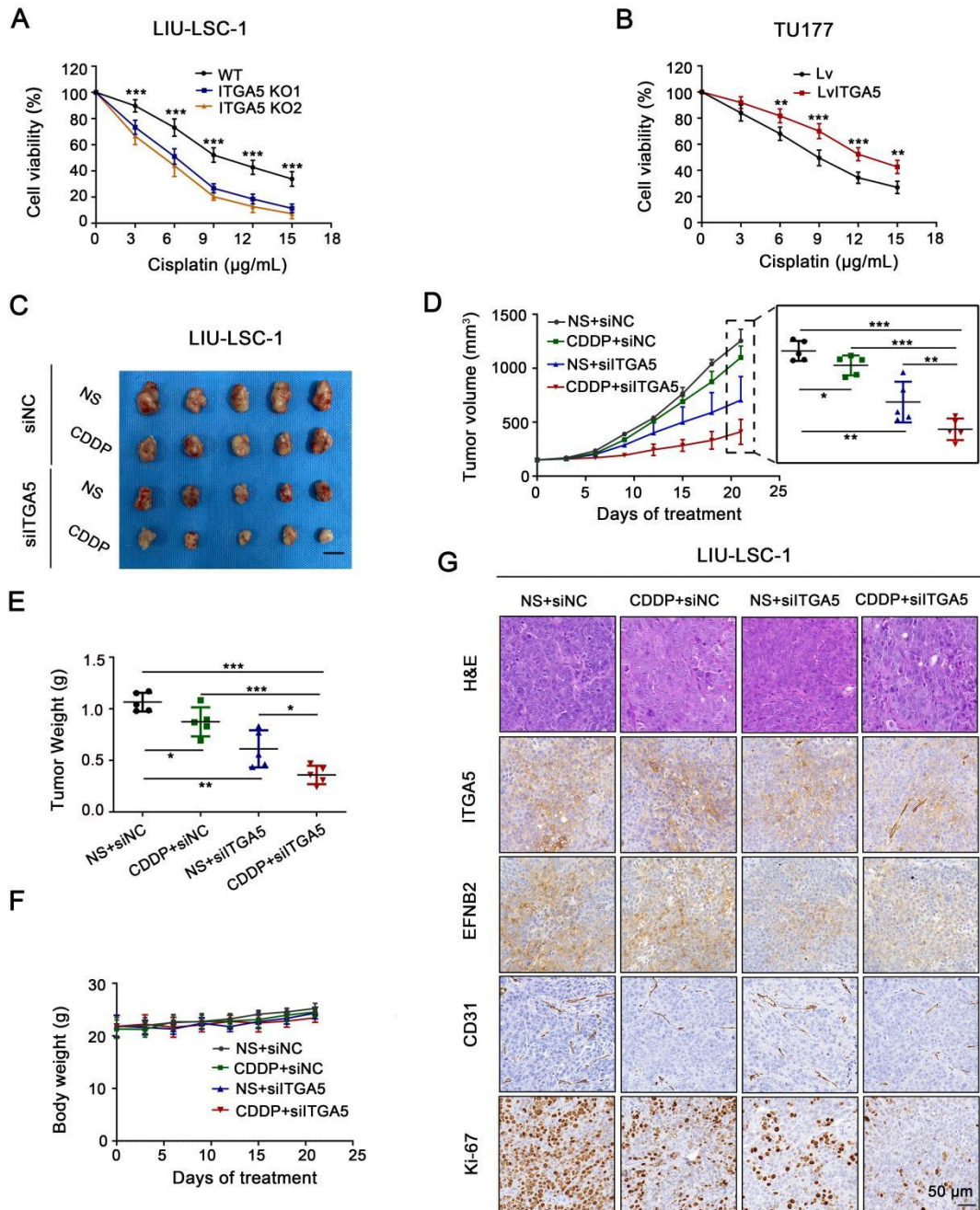


341 **Figure S7. The reduction of proliferation and migration caused by ITGA5**  
342 **knockout were partly rescued by ectopic expression of EFNB2 in LIU-LSC-1**  
343 **cells. (A-B) Proliferative and migratory abilities of EFNB2-overexpressing ITGA5**  
344 **KO LIU-LSC1 cells, empty vector-expressing ITGA5 KO LIU-LSC-1 cells and**  
345 **ITGA5 WT LIU-LSC-1 cells were measured by colony formation (A) and wound**  
346 **healing assays (B), respectively. The error bars represent the mean  $\pm$  SD of triplicate**  
347 **independent experiments. \*\*P < 0.01; \*\*\*P < 0.001.**



349 **Figure S8. The enhancement of LSCC tumor progression mediated by ITGA5**  
 350 **overexpression was attenuated by knockdown of EFNB2. (A-F) EFNB2 shRNA-**  
 351 **(shEFNB2-1) or control shRNA- (shSc) expressing lentiviruses were transduced to**  
 352 **ITGA5-overexpression TU177 cells and control cells. The protein expression of**  
 353 **ITGA5 and EFNB2 were detected by western blotting (A). The cells were subjected**  
 354 **to CCK-8 (B), colony formation (C), wound healing (D), transwell (E) and the CAM**  
 355 **assays (F). (B-E) The error bars represent the mean ± SD of triplicate independent**

356 experiments. \*P < 0.05; \*\*P < 0.01; \*\*\*P < 0.001. Scale Bars, 50  $\mu$ m. **(F)** Error bars  
357 represent mean  $\pm$  SD (n = 6 per group). \*\*P < 0.01; \*\*\*P < 0.001.



359 **Figure S9. Depletion of ITGA5 increases chemosensitivity of CDDP in LSCC**

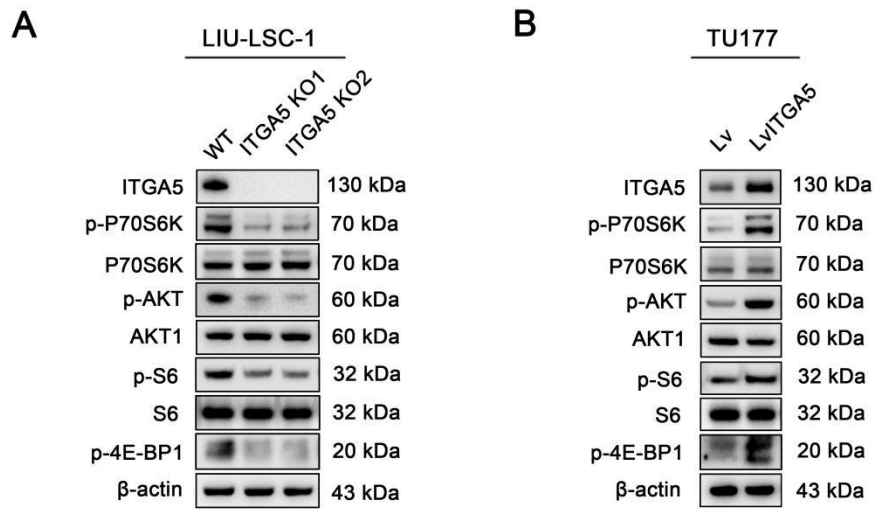
360 **cells. (A-B)** The indicated cells were treated with various concentration of CDDP for

361 24 h, and cell viability was detected with CCK-8 assay. The error bars represent the

362 mean ± SD of triplicate technical replicates. \*\*\*P < 0.001. **(C-G)** Effects of CDDP

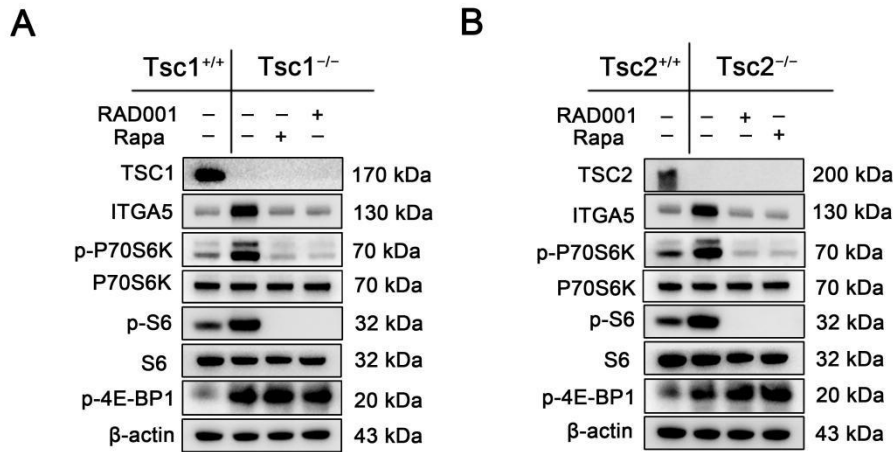
363 combined with ITGA5 siRNAs on LIU-LSC-1 xenograft tumor growth. Tumor

364 images (C), tumor volume (D), tumor weight (E), and body weight of mice (F) were  
365 displayed. Scale bar, 1 cm. Representative IHC images of ITGA5, EFNB2, CD31 and  
366 Ki-67 in subcutaneous xenografts (G). Scale bar, 50  $\mu$ m. Error bars indicate mean  $\pm$   
367 SD (n = 5 mice/group). \*P < 0.05; \*\*P < 0.01; \*\*\*P < 0.001.



369 **Figure S10. ITGA5 positively regulates the activity of AKT and mTORC1 in**  
 370 **LSCC cells. (A-B)** WT and ITGA5 KO LIU-LSC-1 cells **(A)**; ITGA5-overexpressed  
 371 TU177 cells (LvITGA5) and control cells (Lv) **(B)**. Cell lysates were subjected to  
 372 western blotting with the indicated antibodies **(A-B)**.

373 **Figure S11**

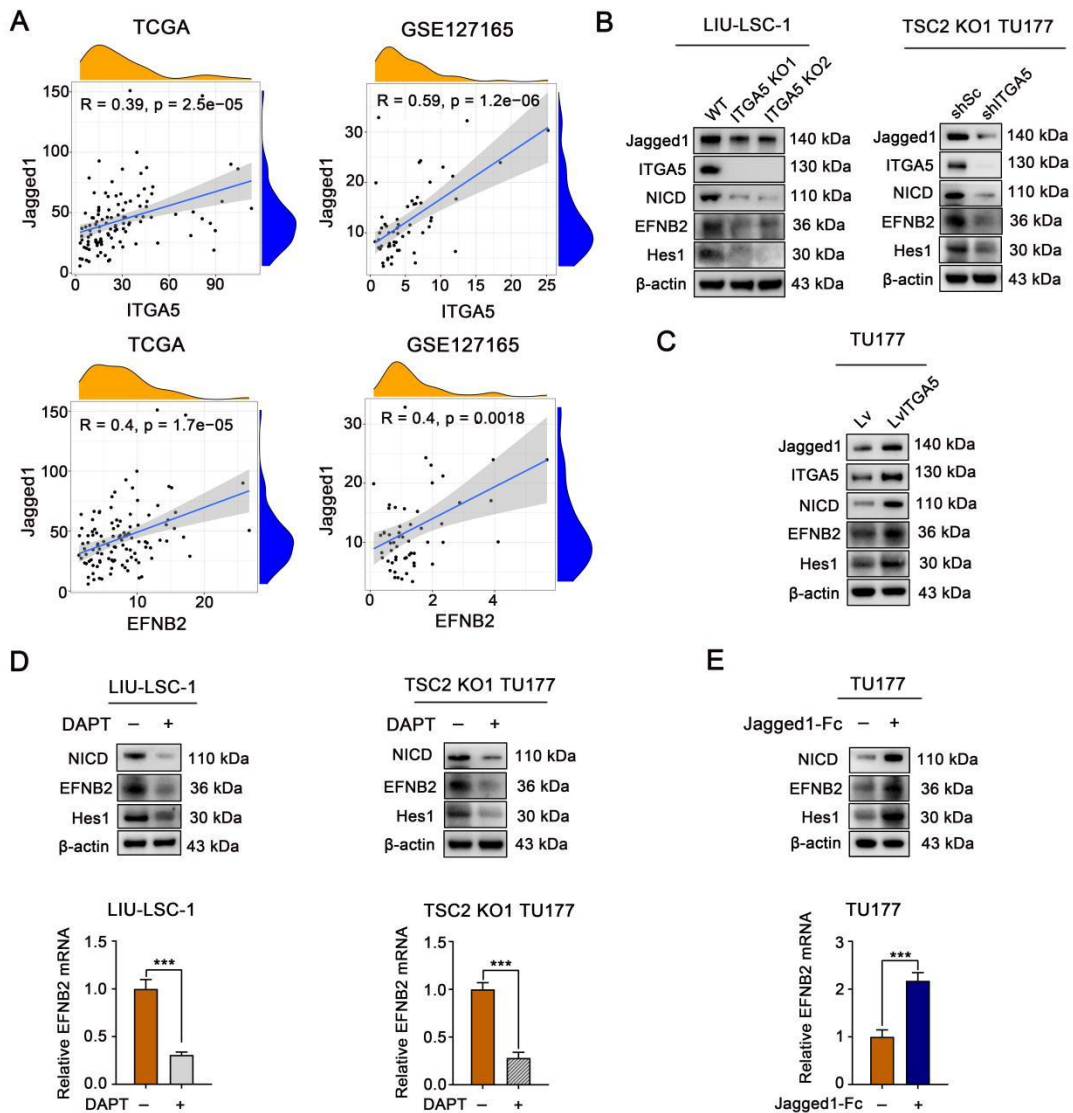


374 **Figure S11. mTORC1 enhances ITGA5 expression in Tsc1<sup>-/-</sup> or Tsc2<sup>-/-</sup> MEFs.**

375 **(A-B)** Tsc1<sup>-/-</sup> **(A)** and Tsc2<sup>-/-</sup> MEFs **(B)** were treated with mTORC1 inhibitors (20

376 nM Rapa or 50 nM RAD001) for 24 h. Cell lysates were subjected to western blot

377 analysis.



379 **Figure S12. ITGA5 upregulates the expression of EFNB2 through the activation**  
 380 **of the Jagged1/Notch1 pathway. (A)** The correlation between Jagged1 and ITGA5  
 381 or EFNB2 expression was analyzed by a Pearson's correlation analysis using the  
 382 TCGA and GSE127165 cohorts. **(B-C)** Cell lysates of the indicated genetically  
 383 engineered LSCC cells were subjected to western blotting with the indicated  
 384 antibodies. **(D-E)** The LIU-LSC-1 and TSC2 KO1 TU177 cells were treated with 10  
 385  $\mu$ M DAPT for 24 h (D); the TU177 cells were treated with 1  $\mu$ g/mL Jagged1-Fc for 24

386 h (**E**). The samples were subjected to western blotting (**upper panel of D and E**) and  
387 qRT-PCR (**lower panel of D and E**) analyses, respectively. The error bars represent  
388 the mean  $\pm$  SD of triplicate technical replicates. \*\*\*P < 0.001.

390 **Table S1. Clinical features of 94 LSCC patients.**

Parameters	Number of Cases (%)
Age	
< 60	34 (36.2)
≥ 60	60 (63.8)
Gender	
Female	9 (9.6)
Male	85 (90.4)
T Stage <sup>1</sup>	
T1	14 (14.9)
T2	22 (23.4)
T3	27 (28.7)
T4	31 (33.0)
lymph node metastasis	
N0	61 (64.9)
N+	33 (35.1)
Distant metastasis	
M0	91 (96.8)
M1	3 (3.2)

<sup>1</sup>TNM Staging is referring to the AJCC 8th edition TNM Staging Criteria.

391 **Table S2. Correlation between p-S6 expression and clinicopathological**  
 392 **characteristics of LSCC patients.**

Characteristic	p-S6 expression		p-value	Method
	High	Low		
n	47	47		
Age, mean ± SD	62.28 ± 12.04	62.21 ± 10.08	0.978	T test
Gender, n (%)			1.000	Fisher.test
Female	5 (5.3%)	4 (4.3%)		
Male	42 (44.7%)	43 (45.7%)		
T Stage, n (%)			< 0.001	Chisq.test
T1	4 (4.3%)	10 (10.6%)		
T2	5 (5.3%)	17 (18.1%)		
T3	13 (13.8%)	14 (14.9%)		
T4	25 (26.6%)	6 (6.4%)		
Lymph node metastasis, n (%)			0.006	Fisher.test
N0	23 (24.5%)	38 (40.4%)		
N1	5 (5.3%)	3 (3.2%)		
N2	14 (14.9%)	3 (3.2%)		
N3	5 (5.3%)	3 (3.2%)		
Distant metastasis, n (%)			1.000	Fisher.test
M0	46 (48.9%)	45 (47.9%)		
M1	1 (1.1%)	2 (2.1%)		

393 **Table S3. Correlation between ITGA5 expression and clinicopathological**  
 394 **characteristics of LSCC patients.**

Characteristic	ITGA5 expression		p-value	Method
	High	Low		
n	47	47		
Age, mean ± SD	62.49 ± 12.18	62 ± 9.91	0.831	T test
Gender, n (%)			1.000	Fisher.test
Female	4 (4.3%)	5 (5.3%)		
Male	43 (45.7%)	42 (44.7%)		
T Stage, n (%)			< 0.001	Chisq.test
T1	4 (4.3%)	10 (10.6%)		
T2	4 (4.3%)	18 (19.1%)		
T3	12 (12.8%)	15 (16%)		
T4	27 (28.7%)	4 (4.3%)		
Lymph node metastasis, n (%)			< 0.001	Fisher.test
N0	21 (22.3%)	40 (42.6%)		
N1	5 (5.3%)	3 (3.2%)		
N2	14 (14.9%)	3 (3.2%)		
N3	7 (7.4%)	1 (1.1%)		
Distant metastasis, n (%)			1.000	Fisher.test
M0	45 (47.9%)	46 (48.9%)		
M1	2 (2.1%)	1 (1.1%)		

395 **Table S4. Correlation between EFNB2 expression and clinicopathological**  
 396 **characteristics of LSCC patients.**

Characteristic	EFNB2 expression		p	Method
	High	Low		
n	47	47		
Age, mean $\pm$ SD	61.64 $\pm$ 11.01	62.85 $\pm$ 11.17	0.597	T test
Gender, n (%)			1.000	Fisher.test
Female	5 (5.3%)	4 (4.3%)		
Male	42 (44.7%)	43 (45.7%)		
T Stage, n (%)			< 0.001	Chisq.test
T1	7 (7.4%)	7 (7.4%)		
T2	6 (6.4%)	16 (17%)		
T3	9 (9.6%)	18 (19.1%)		
T4	25 (26.6%)	6 (6.4%)		
Lymph node metastasis, n (%)			0.025	Fisher.test
N0	24 (25.5%)	37 (39.4%)		
N1	4 (4.3%)	4 (4.3%)		
N2	13 (13.8%)	4 (4.3%)		
N3	6 (6.4%)	2 (2.1%)		
Distant metastasis, n (%)			1.000	Fisher.test
M0	45 (47.9%)	46 (48.9%)		
M1	2 (2.1%)	1 (1.1%)		

397 **Table S5. STR analysis of LIU-LSC-1 cell line.**

STR alleles	LIU-LSC-1 cell line	
	Allele1	Allele2
D5S818	12	
D13S317	8	
D7S820	8	11
D16S539	11	
VWA	16	
TH01	8	
AMEL	X	Y
TPOX	8	11
CSF1PO	10	12
D12S391	15	22
FGA	23	
D2S1338	21	23
D21S11	29	
D18S51	20	
D8S1179	13	14
D3S1358	16	
D6S1043	11	12
PENTAE	16	22
D19S433	15.2	16.2
PENTAD	13	

398 **Table S6. Cell lines and growth medium.**

Cell line	Source	Tissue source	Complete growth medium
TU177	Otwo Biotech Inc. (Shenzhen, China).	laryngeal SCC	RPMI 1640 (Gibco: Cat# 11875093) + 10% FBS (Biological Industries, Cat# 04-001-1ACS) + 1% penicillin/streptomycin (Beyotime, Cat# C0222) Epithelial Cell Complete Medium (VivaCell: Cat# C3660-0100) + 1% penicillin/streptomycin (Beyotime, Cat# C0222)
LIU-LSC-1	newly established cell line	laryngeal SCC	RPMI 1640 (Gibco: Cat# 11875093) + 10% FBS (Biological Industries, Cat# 04-001-1ACS) + 1% penicillin/streptomycin (Beyotime, Cat# C0222) DMEM (Gibco: Cat# 11995065) + 10% FBS
AMC-HN-8	Otwo Biotech Inc. (Shenzhen, China).	laryngeal SCC	(Biological Industries, Cat# 04-001-1ACS) + 1% penicillin/streptomycin (Beyotime, Cat# C0222) DMEM (Gibco: Cat# 11995065) + 10% FBS
Tsc1 <sup>+/+</sup>	described previously	Murine embryonic fibroblasts (MEFs)	(Biological Industries, Cat# 04-001-1ACS) + 1% penicillin/streptomycin (Beyotime, Cat# C0222) DMEM (Gibco: Cat# 11995065) + 10% FBS
Tsc1 <sup>-/-</sup>	described previously	Murine embryonic fibroblasts (MEFs)	(Biological Industries, Cat# 04-001-1ACS) + 1% penicillin/streptomycin (Beyotime, Cat# C0222) DMEM (Gibco: Cat# 11995065) + 10% FBS
Tsc2 <sup>+/+</sup>	described previously	Murine embryonic fibroblasts (MEFs)	(Biological Industries, Cat# 04-001-1ACS) + 1% penicillin/streptomycin (Beyotime, Cat# C0222) DMEM (Gibco: Cat# 11995065) + 10% FBS
Tsc2 <sup>-/-</sup>	described previously	Murine embryonic fibroblasts (MEFs)	(Biological Industries, Cat# 04-001-1ACS) + 1% penicillin/streptomycin (Beyotime, Cat# C0222)
HEK293T	ATCC (Manassas,	kidney; Embryo	DMEM (Gibco: Cat#

VA,USA)

11995065) + 10% FBS  
(Biological Industries, Cat#  
04-001-1ACS + 1%  
penicillin/streptomycin  
(Beyotime, Cat# C0222)

---

399 **Table S7. Detailed information of antibodies.**

ANDIBODYS	SOURCE	IDENTIFIER
Mouse monoclonal antibody anti-Ki-67	Cell Signaling Technology	Cat# 9027S
Mouse monoclonal antibody anti-beta-Actin	Sigma-Aldrich	Cat# A1978
Rabbit monoclonal antibody anti-ITGA5	Abcam	Cat# ab150361
Rabbit monoclonal antibody anti-EFNB2	Sigma-Aldrich	Cat# HPA008999
Rabbit monoclonal antibody anti-HIF-1 $\alpha$	Abcam	Cat# ab228649
Rabbit monoclonal antibody anti-p-S6 (S235/236)	Cell Signaling Technology	Cat# 4857S
Rabbit monoclonal antibody anti-S6	Cell Signaling Technology	Cat# 2217S
Rabbit monoclonal antibody anti-mTOR	Cell Signaling Technology	Cat# 2983P
Rabbit monoclonal antibody anti-Rictor	Cell Signaling Technology	Cat# 2114S
Rabbit monoclonal antibody anti-Raptor	Cell Signaling Technology	Cat# 2280S
Rabbit monoclonal antibody anti-CD31	Abcam	Cat# ab76533
Goat Anti-Rabbit IgG H&L (FITC)	Abcam	Cat# ab6717
Goat Anti-Mouse IgG HRP	Abcam	Cat# ab6789
Goat Anti-Rabbit IgG HRP	Abcam	Cat# ab6721
Mouse monoclonal antibody anti-CD44	Abcam	Cat# ab6124
Rabbit monoclonal antibody anti- Jagged1	Abcam	Cat# ab109536
Rabbit monoclonal antibody anti-p-mTOR(S2448)	Cell Signaling Technology	Cat# 5536S
Rabbit monoclonal antibody anti-TSC1	Cell Signaling Technology	Cat# 6935S
Rabbit monoclonal antibody anti-TSC2	Cell Signaling Technology	Cat# 4308S
Rabbit monoclonal antibody anti-p-AKT(S473)	Cell Signaling Technology	Cat# 4060S

Rabbit monoclonal antibody anti-AKT1	Cell Signaling Technology	Cat# 75692S
Rabbit monoclonal antibody anti-NICD	Cell Signaling Technology	Cat# 4147S
Rabbit monoclonal antibody anti-p-4E-BP1 (T37/46)	Cell Signaling Technology	Cat# 2855S
Rabbit monoclonal antibody anti-Hes1	Abcam	Cat#ab108937
Rabbit polyclonal antibody anti-P70S6K (phospho T389)	Abcam	Cat# ab2571
Rabbit monoclonal antibody anti-P70S6K	Abcam	Cat# ab32529

---

400 **Table S8. Primer information for qRT-PCR analysis.**

Primer name	GC content (%)	Tm (°C)	Annealing Temperature (°C)	Primer sequence
β-actin FORWARD	52.2	58.5	60	CTG GCA CCA CAC CTT CTA CAA TG
β-actin REVERSE	61.9	61.3		GGC GTA CAG GGA TAG CAC AGC
ITGA5 FORWARD	45.5	54.6	60	CAT GAT GAG TTT GGC CGA TTT G
ITGA5 REVERSE	45.5	54.2		CCC CCA GGA AAT ACA AAC ACT A
EFNB2 FORWARD	40.9	53.2	60	TAA AGA TCC AAC AAG ACG TCC A
EFNB2 REVERSE	45.5	53.3		CGT GAT GAT GAT GAC GAT GAA G
RAPTOR FORWARD	50.0	56.0	60	GAC ACG GAA GAT GTT CGA CAA G
RAPTOR REVERSE	50.0	54.7		ATC TGA GAA GCA ACG CTC TC

401 **Table S9.** Differentially expressed genes of the RNA-seq (shRaptor-1 LIU-LSC-1  
402 cells vs. shSc LIU-LSC-1 cells).

403 **Table S10.** The top 10 enriched pathways of down-regulated differentially expressed  
404 genes in shRaptor-1 LIU-LSC-1 cells compared to the control cells (shSc LIU-LSC-1  
405 cells).

406 **Table S11.** Differentially expressed genes of the RNA-seq (ITGA5 KO2 LIU-LSC-1  
407 cells vs. WT LIU-LSC-1 cells).